

Search for 14.4 keV solar axions from M1 transition of ^{57}Fe with CUORE crystals

F. Alessandria,¹ **R. Ardito,**² **D. R. Artusa,**^{3,4} **F. T. Avignone III,**³ **O. Azzolini,**⁵ **M. Balata,**⁴ **T. I. Banks,**^{4,6,7} **G. Bari,**⁸ **J. Beeman,**⁹ **F. Bellini,**^{10,11} **A. Bersani,**¹² **M. Biassoni,**^{13,14} **T. Bloxham,**⁷ **C. Brofferio,**^{13,14} **C. Bucci,**⁴ **X. Z. Cai,**¹⁵ **L. Canonica,**⁴ **S. Capelli,**^{13,14} **L. Carbone,**¹⁴ **L. Cardani,**^{10,11} **M. Carrettoni,**^{13,14} **N. Casali,**⁴ **N. Chott,**³ **M. Clemenza,**^{13,14} **C. Cosmelli,**^{10,11} **O. Cremonesi,**^{*14} **R. J. Creswick,**³ **I. Dafinei,**¹¹ **A. Dally,**¹⁶ **V. Datsovov,**¹⁴ **A. De Biasi,**⁵ **M. P. Decowski,**^{#6,7} **M. M. Deninno,**⁸ **S. Di Domizio,**^{12,17} **M. L. di Vacri,**⁴ **L. Ejzak,**¹⁶ **R. Faccini,**^{10,11} **D. Q. Fang,**¹⁵ **H. A. Farach,**³ **E. Ferri,**^{13,14} **F. Ferroni,**^{10,11} **E. Fiorini,**^{13,14} **M. A. Franceschi,**¹⁸ **S. J. Freedman,**^{6,7} **B. K. Fujikawa,**⁷ **A. Giachero,**¹⁴ **L. Gironi,**^{13,14} **A. Giuliani,**¹⁹ **J. Goett,**⁴ **P. Gorla,**²⁰ **C. Gotti,**^{13,14} **E. Guardincerri,**^{‡4,7} **T. D. Gutierrez,**²¹ **E. E. Haller,**^{9,22} **K. Han,**⁷ **K. M. Heeger,**¹⁶ **H. Z. Huang,**²³ **R. Kadel,**²⁴ **K. Kazkaz,**²⁵ **G. Keppel,**⁵ **L. Kogler,**^{§6,7} **Yu. G. Kolomensky,**^{6,24} **D. Lenz,**¹⁶ **Y. L. Li,**¹⁵ **C. Ligi,**¹⁸ **X. Liu,**²³ **Y. G. Ma,**¹⁵ **C. Maiano,**^{13,14} **M. Maino,**^{13,14} **M. Martinez,**²⁶ **R. H. Maruyama,**¹⁶ **N. Moggi,**⁸ **S. Morganti,**¹¹ **T. Napolitano,**¹⁸ **S. Newman,**^{3,4} **S. Nisi,**⁴ **C. Nones,**²⁷ **E. B. Norman,**^{25,28} **A. Nucciotti,**^{13,14} **F. Orio,**¹¹ **D. Orlandi,**⁴ **J. L. Ouellet,**^{6,7} **M. Pallavicini,**^{12,17} **V. Palmieri,**⁵ **L. Pattavina,**¹⁴ **M. Pavan,**^{13,14} **M. Pedretti,**²⁵ **G. Pessina,**¹⁴ **S. Pirro,**¹⁴ **E. Previtali,**¹⁴ **V. Rampazzo,**⁵ **F. Rimondi,**^{†8,29} **C. Rosenfeld,**³ **C. Rusconi,**¹⁴ **S. Sangiorgio,**²⁵ **N. D. Scielzo,**²⁵ **M. Sisti,**^{13,14} **A. R. Smith,**³⁰ **F. Stivanello,**⁵ **L. Taffarello,**³¹ **M. Tenconi,**¹⁹ **W. D. Tian,**¹⁵ **C. Tomei,**¹¹ **S. Trentalange,**²³ **G. Ventura,**^{32,33} **M. Vignati,**¹¹ **B. S. Wang,**^{25,28} **H. W. Wang,**¹⁵ **C. A. Whitten Jr.,**^{‡23} **T. Wise,**¹⁶ **A. Woodcraft,**³⁴ **L. Zanotti,**^{13,14} **C. Zarra,**⁴ **B. X. Zhu,**²³ **S. Zucchelli**^{§8,29} **(The CUORE Collaboration)**

¹INFN - Sezione di Milano, Milano I-20133 - Italy

²Dipartimento di Ingegneria Strutturale, Politecnico di Milano, Milano I-20133 - Italy

³Department of Physics and Astronomy, University of South Carolina, Columbia, SC 29208 - USA

⁴INFN - Laboratori Nazionali del Gran Sasso, Assergi (L'Aquila) I-67010 - Italy

⁵INFN - Laboratori Nazionali di Legnaro, Legnaro (Padova) I-35020 - Italy

⁶Department of Physics, University of California, Berkeley, CA 94720 - USA

⁷Nuclear Science Division, Lawrence Berkeley National Laboratory, Berkeley, CA 94720 - USA

⁸INFN - Sezione di Bologna, Bologna I-40127 - Italy

⁹Materials Science Division, Lawrence Berkeley National Laboratory, Berkeley, CA 94720 - USA

¹⁰Dipartimento di Fisica, Sapienza Università di Roma, Roma I-00185 - Italy

¹¹INFN - Sezione di Roma, Roma I-00185 - Italy

*Corresponding author: cuore-spokesperson@lngs.infn.it

#Presently at: Nikhef, 1098 XG Amsterdam - The Netherlands

‡Presently at: Los Alamos National Laboratory, Los Alamos, NM 87545 - USA

§Presently at: Sandia National Laboratories, Livermore, CA 94551 - USA

†deceased

¹²INFN - Sezione di Genova, Genova I-16146 - Italy

¹³Dipartimento di Fisica, Università di Milano-Bicocca, Milano I-20126 - Italy

¹⁴INFN - Sezione di Milano Bicocca, Milano I-20126 - Italy

¹⁵Shanghai Institute of Applied Physics (Chinese Academy of Sciences), Shanghai 201800 - China

¹⁶Department of Physics, University of Wisconsin, Madison, WI 53706 - USA

¹⁷Dipartimento di Fisica, Università di Genova, Genova I-16146 - Italy

¹⁸INFN - Laboratori Nazionali di Frascati, Frascati (Roma) I-00044 - Italy

¹⁹Centre de Spectrométrie Nucléaire et de Spectrométrie de Masse, 91405 Orsay Campus - France

²⁰INFN - Sezione di Roma Tor Vergata, Roma I-00133 - Italy

²¹Physics Department, California Polytechnic State University, San Luis Obispo, CA 93407 - USA

²²Department of Materials Science and Engineering, University of California, Berkeley, CA 94720 - USA

²³Department of Physics and Astronomy, University of California, Los Angeles, CA 90095 - USA

²⁴Physics Division, Lawrence Berkeley National Laboratory, Berkeley, CA 94720 - USA

²⁵Lawrence Livermore National Laboratory, Livermore, CA 94550 - USA

²⁶Laboratorio de Fisica Nuclear y Astroparticulas, Universidad de Zaragoza, Zaragoza 50009 - Spain

²⁷Service the Physique des Particules, CEA/Saclay, 91191 Gif-sur-Yvette - France

²⁸Department of Nuclear Engineering, University of California, Berkeley, CA 94720 - USA

²⁹Dipartimento di Fisica, Università di Bologna, Bologna I-40127 - Italy

³⁰EH&S Division, Lawrence Berkeley National Laboratory, Berkeley, CA 94720 - USA

³¹INFN - Sezione di Padova, Padova I-35131 - Italy

³²Dipartimento di Fisica, Università di Firenze, Firenze I-50125 - Italy

³³INFN - Sezione di Firenze, Firenze I-50125 - Italy

³⁴SUPA, Institute for Astronomy, University of Edinburgh, Blackford Hill, Edinburgh EH9 3HJ - UK

Abstract. We report the results of a search for axions from the 14.4 keV M1 transition from ^{57}Fe in the core of the sun using the axio-electric effect in TeO_2 bolometers. The detectors are $5 \times 5 \times 5 \text{ cm}^3$ crystals operated at about 10 mK in a facility used to test bolometers for the CUORE experiment at the Laboratori Nazionali del Gran Sasso in Italy. An analysis of 43.65 kg·d of data was made using a newly developed low energy trigger which was optimized to reduce the detectors energy threshold. An upper limit of $0.63 \text{ c} \cdot \text{kg}^{-1} \cdot \text{d}^{-1}$ was established at 95% C.L.. From this value, a lower bound at 95% C.L. was placed on the Peccei-Quinn energy scale of $f_a \geq 0.76 \times 10^6 \text{ GeV}$ for a value of $S=0.55$ for the flavor-singlet axial vector matrix element. Bounds are given for the interval $0.15 \leq S \leq 0.55$.

Contents

1	Introduction	1
2	Experiment	3
3	Results	5
4	Summary and Conclusions	7
5	Acknowledgments	7

1 Introduction

Quantum chromodynamics or QCD, largely accepted as the best theory describing strong interactions, contains one curious blemish known as “the strong CP problem”. QCD predicts a large neutron electric dipole moment, of the order $|d_n| \approx 10^{-16}$ e·cm, whereas the experimental bound is $|d_n| \leq 2.9 \times 10^{-26}$ e·cm [1]. This fact puts an unnaturally small upper limit ($< 10^{-10}$) to the θ_{QCD} parameter, the strength of the CP violating term present in the QCD. In order to explain this small value Roberto Peccei and Helen Quinn proposed [2] that the QCD Lagrangian possessed an additional global U(1) symmetry which modified the CP-violating term to:

$$\mathcal{L}_\theta = (\theta_{QCD} - \frac{a}{f_a}) \frac{g_s^2}{32\pi^2} G_a^{\mu\nu} \tilde{G}_{a\mu\nu}. \quad (1.1)$$

where g_s is the strong coupling constant, $G_a^{\mu\nu}$ the gluon field, a a new scalar field, and f_a an energy scale. Non-perturbative effects induce a potential for the field a that has a minimum at $a = f_a \theta_{QCD}$ which causes the spontaneous breaking of the global U(1) symmetry. As later shown by Weinberg and Wilczek [3], the spontaneous breaking symmetry produces a Nambu-Goldstone boson known as the axion.

The “standard” Peccei-Quinn axion with symmetry breaking scale of the order of the electro-weak scale is ruled out by experiments. However, other models of “invisible” axions which break the symmetry at much higher energies are still an interesting possibility, and the search of an axion mass in the range between $10^{-10} - 10^{-6}$ eV is a very active field of research. The possibility that the axion might be most or part of the dark-matter has reinforced even further the interest for this field [4].

The most common models are the so called hadronic or KSVZ axion model [5] and the GUT or DFSZ models [6]. In both cases, the mass of the axion is directly related to the axion’s decay constant, f_a , the pion’s mass $m_\pi = 135$ MeV, the pion’s decay constant $f_\pi \approx 92$ MeV, and the up-down quark mass ratio, $z = 0.56$ [7], as follows:

$$m_a = \left(\frac{z}{(1+z+w)(1+z)} \right)^{\frac{1}{2}} \frac{f_\pi m_\pi}{f_a} = 6 \text{ [eV]} \left(\frac{10^6}{f_a \text{ [GeV]}} \right). \quad (1.2)$$

where $w = m_u/m_s = 0.029$.

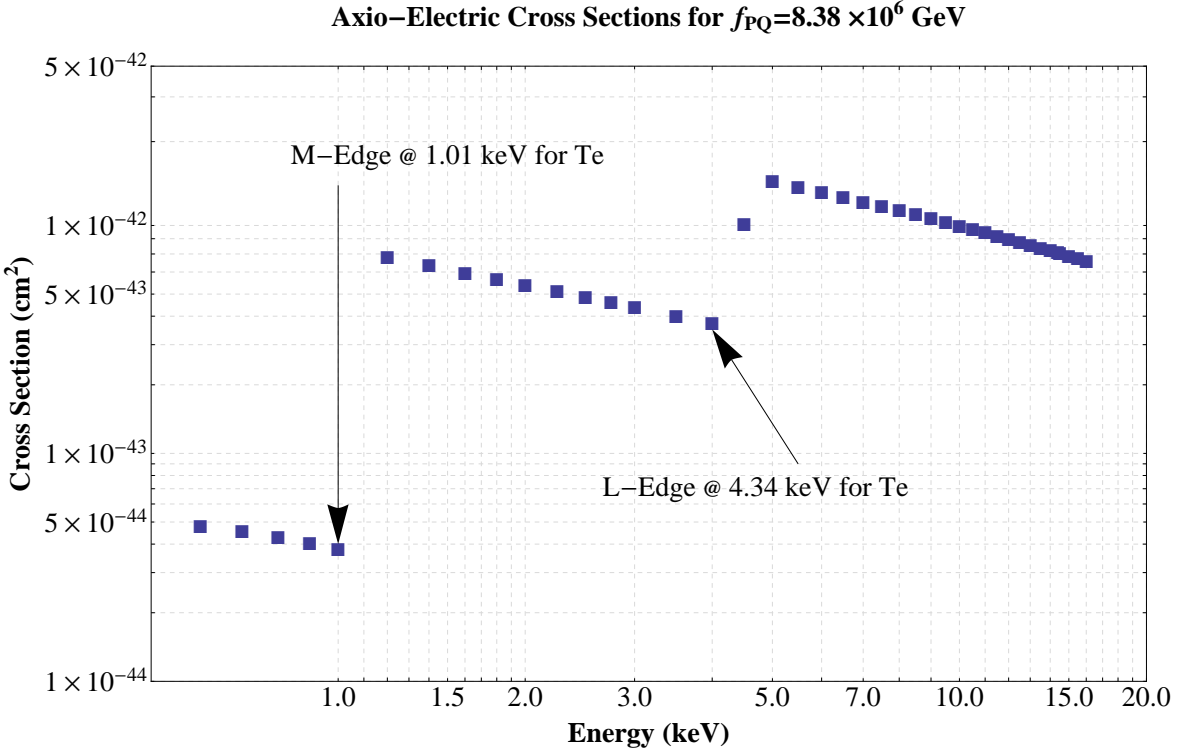


Figure 1. Axio-electric cross sections of TeO_2 in the energy range 0-20 keV using $f_a=8.38 \times 10^6$ GeV.

26 The detection mechanism used in the present work is the axio-electric effect, which is
 27 the equivalent of a photo-electric effect with the absorption of an axion instead of a photon.
 28 The cross section, which can be seen in Fig. 1 for TeO_2 , is given by [8]:

$$\sigma_{ae} = \frac{\alpha_{axion}}{2\alpha_{EM}} \left(\frac{\hbar\omega}{m_e c^2} \right)^2 \sigma_{pe} \quad (1.3)$$

$$\text{with, } \alpha_{axion} = \frac{1}{4\pi} \left(\frac{2x'_e m_e c^2}{f_a} \right)^2. \quad (1.4)$$

29 For Eq. 1.4, $x'_e \approx 1$, $m_e c^2$ is the electron mass in GeV, $\alpha_{EM} = \frac{1}{137}$, and σ_{pe} is the photo-
 30 electric cross sections for each element (taken from [9]).

31 The axion source in this search is the M1 transition produced by thermal excitation of
 32 ^{57}Fe in the solar core. The isotope ^{57}Fe is stable and has 2.12% natural abundance, yielding
 33 an average ^{57}Fe density in the Sun's core of $(9.0 \pm 1.2) 10^{19} \text{ cm}^{-3}$. The uncertainty is mostly
 34 due to the different metal diffusion models in the core and is computed in [10]. The first
 35 excited state is at 14.4 keV, low enough to be thermally excited in the interior of the sun,
 36 which has an average temperature $kT \approx 1.3 \text{ keV}$ [11][12].

37 In this paper we rely on [12] for the determination of the expected axion flux and axion
 38 interaction rate in TeO_2 crystals. The 15% error in the knowledge of ^{57}Fe density is taken
 39 into account.

40 The Lagrangian that couples axions to nucleons is:

$$\mathcal{L} = a\bar{\psi}_i \gamma_5 (g_0 \beta + g_3 \tau_3) \psi. \quad (1.5)$$

Table 1. Detection Rates for TeO_2 (counts· $\text{kg}^{-1}\cdot\text{d}^{-1}$)

$S \setminus f_a(\text{GeV})$	3.0×10^5	5.0×10^5	7.0×10^5	9.0×10^5	1.1×10^6
0.15	0.070	0.014	0.007	0.00273	0.00122
0.20	0.349	0.069	0.037	0.0136	0.00609
0.25	0.840	0.166	0.089	0.0327	0.01466
0.30	1.542	0.304	0.164	0.0601	0.02694
0.35	2.457	0.485	0.262	0.0958	0.04293
0.40	3.585	0.707	0.382	0.140	0.06263
0.45	4.924	0.972	0.525	0.192	0.08604
0.50	6.476	1.278	0.690	0.253	0.11316
0.55	8.241	1.627	0.878	0.321	0.14398

⁴¹ Here, g_0 and g_3 are the iso-scalar and iso-vector coupling constants, and τ_3 is a Pauli matrix.
⁴² The axion-nucleon coupling constants are defined by [12]:

$$g_0 = -7.8 \times 10^{-8} \left(\frac{6.2 \times 10^6 \text{GeV}}{f_a} \right) \left(\frac{3F - D + 2S}{3} \right) \quad (1.6)$$

$$g_3 = -7.8 \times 10^{-8} \left(\frac{6.2 \times 10^6 \text{GeV}}{f_a} \right) \left((D + F) \frac{1 - z}{1 + z} \right) \quad (1.7)$$

⁴³ where $F \approx 0.48$ and $D = 0.77$ are invariant matrix elements of the axial current [13]. The Spin-
⁴⁴ Muon Collaboration lists a range for S of $0.15 \leq S \leq 0.50$ at 95% C.L [14] while Altarelli *et.*
⁴⁵ *al* give the range $0.37 \leq S \leq 0.53$ [15]. Both g_0 and g_3 contribute to the axion branching ratio.
⁴⁶ This is critical to the formulation of the energy loss within the sun due to axion emission.
⁴⁷ Combined with the flux rates listed in Ref. [8] the axion detection rates were determined and
⁴⁸ listed Table 1.

49 2 Experiment

50 In the analysis shown in the present work we will focus on the results from a specific R&D
⁵¹ run dedicated to the CUORE experiment.

52 CUORE will be an array of 988 tellurium dioxide crystals, each with size $5 \times 5 \times 5 \text{ cm}^3$
⁵³ and weight 750 grams, which will be operated as bolometers at a temperature of about 10 mK
⁵⁴ to search for neutrino-less double beta decay of ^{130}Te and other rare events. A description of
⁵⁵ the CUORE technique and the basic principles behind bolometers is given in [16], [17], [18],
⁵⁶ and [19].

57 The crystals to be used for CUORE are produced at the Shanghai Institute for Ceramics
⁵⁸ of the Chinese Academy of Science (SICCAS), and are shipped to the Laboratori Nazionali
⁵⁹ del Gran Sasso (LNGS) located in Assergi, Italy. The crystals are produced and shipped
⁶⁰ in batches to LNGS. Four crystals are taken at random from each batch to measure their
⁶¹ radioactive contamination levels and evaluate their performance at low temperature. Each
⁶² one of these runs is called a Cuore Crystal Validation Run, or CCVR [20]. This paper will
⁶³ analyze data from the second run, known as CCVR2.

64 The four TeO_2 crystals have a total active mass of 3 kg and are mounted in a specially
⁶⁵ designed copper frame which is placed inside a dilution refrigerator at LNGS. The cryostat

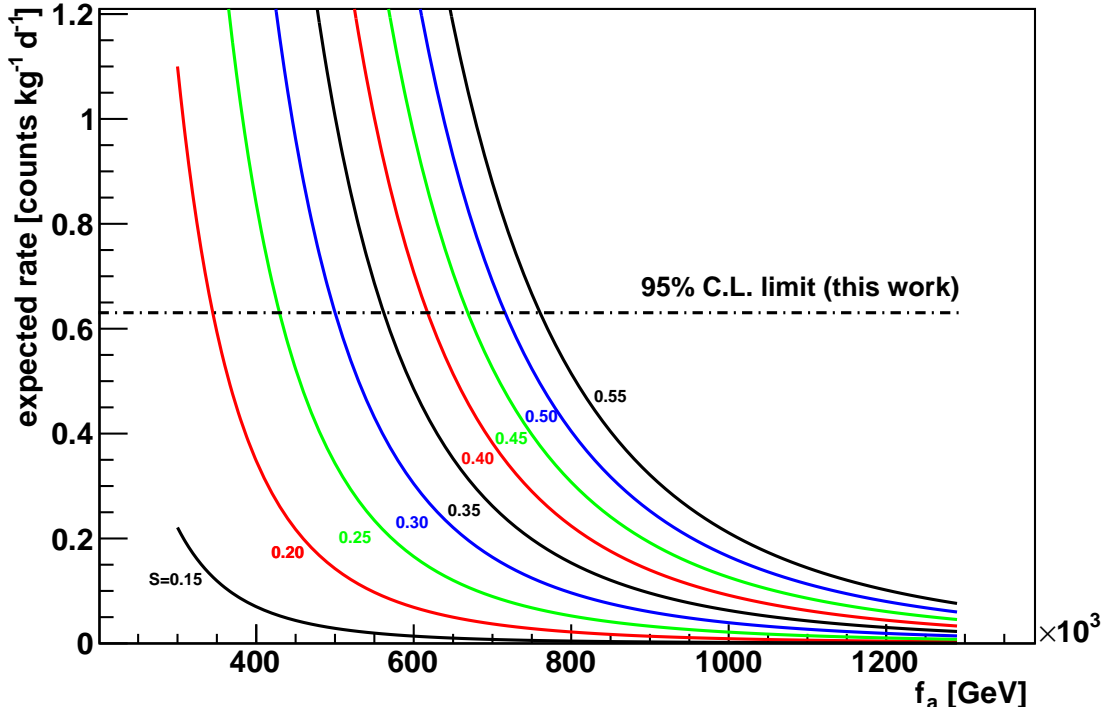


Figure 2. Expected rate in the axion region as a function of the f_a axion constant for different values of the nuclear S parameter. The horizontal line indicates the upper limit obtained in this work.

66 is maintained at a working temperature of approximately 8-10 mK throughout the runs
 67 duration.

68 Attached to each CCVR crystal are two neutron transmutation doped germanium semi-
 69 conductors, NTDs. CCVR2 collected data for a total of 19.4 days for a total of 43.65 kg·d.
 70 Calibrations were performed in the middle and end of the run with a ^{232}Th γ source inserted
 71 inside the Pb shielding, close to the cryostat outer vacuum vessel.

72 Previous CUORE R&D experiments, such as CUORICINO [16][21], had bolometers
 73 whose typical threshold was 50 keV. Since the Q-value for ^{130}Te is at 2527 keV [22][23], a
 74 threshold at 50 keV was more than satisfactory for $\beta\beta$ -decay searches. However, to investigate
 75 physical events at lower energies, new procedures were needed to lower the energy threshold.
 76 For this reason a special low-energy trigger was developed and applied offline, exploiting the
 77 fact that the standard CUORE DAQ used in the CCVR runs collects data continuously and
 78 with no hardware trigger using 125 Hz 18-bits digitizers [24].

79 This trigger algorithm maximizes the signal to noise ratio by filtering the data with a
 80 known power spectrum and a reference signal shape. A full description of it is given in [25].
 81 More details can be found in [26].

82 **3 Results**

83 In order to reject thermal and microphonic noise, the pulses are selected by applying cuts on
 84 the pulse shape parameters. The efficiency of these cuts must therefore be taken into account
 85 in the analysis. As usually done in Cuoricino and in all CCVR runs, a calibrated current
 86 pulse is sent every 30 minutes to a small resistor (heater) that is glued on each crystal. This
 87 calibration pulse is used to correct for temperature variations in the cryostat that change the
 88 response of the bolometer and therefore its signal amplitude. It is also used to measure the
 89 detection efficiency of the crystals.

90 The detection efficiencies (ϵ_D) were measured using the heaters [27][28][29] through a
 91 dedicated measurement performed at the end of the data-taking. The equivalence of the
 92 bolometers response to particle and heater pulses was demonstrated via a MonteCarlo simu-
 93 lation [30] that allows to infer ϵ_D for the bolometer without the heater. Since the detection
 94 capability may vary with time, the fluctuation of the peak rate with time (11%) of the low-
 95 est energy γ line (a 4.7 keV line described below) can be used as an (over)estimate of the
 96 systematic error on the detection efficiency [26].

97 The estimated values of ϵ_D are 0.91 ± 0.10 for B1 and 0.83 ± 0.09 for B2 and B3,
 98 dominated by the systematics. The pulse shape cut efficiencies have been evaluated on the
 99 4.7 keV peak and are equal to 1.

100 The low energy spectrum, below 50 keV, is shown in Fig. 3. For this work we choose
 101 to include only the channels whose thresholds are lower than 5 keV as to include the peak
 102 at 4.7 keV. The physical interpretation of this peak is still being analyzed, but the lack of a
 103 full understanding of its origin has no consequence on the present work, because we used its
 104 width only to determine the energy resolution in the 14.4 KeV region.

105 Energy calibration in this very low energy region is not done with the ^{232}Th lines, which
 106 are normally used for higher energy studies. The energy region between 2.5 and 300 keV is
 107 calibrated using a set of metastable Te lines that result from cosmogenic activation. The
 108 crystals spend a few weeks above ground while they are being shipped by sea¹ between the
 109 production site in Shanghai, China and arrival at the underground storage site at LNGS. The
 110 main lines used in the calibration for present work are reported in Table 2.

Energy [keV]	Source	Life-Time (days)
30.4912	Sb X-ray	–
88.26 ± 0.08	^{127m}Te	109 ± 2
105.50 ± 0.05	^{129m}Te	33.6 ± 0.1
144.78 ± 0.03	^{125m}Te	57.40 ± 0.15
247.5 ± 0.2	^{123m}Te	119.7 ± 0.1
293.98 ± 0.04	^{121m}Te	154 ± 7

Table 2. List of γ lines from meta-stable Te isotopes used in this analysis for the energy calibration in the energy region between 2.5 and 300 keV. The lines are available from cosmogenic activation of Te during shipment, and have half-lives spanning from 33.6 days and 119.7 days.

¹The shipment of two (out of four) crystals was actually made by airplane, which induces a slightly higher activation.

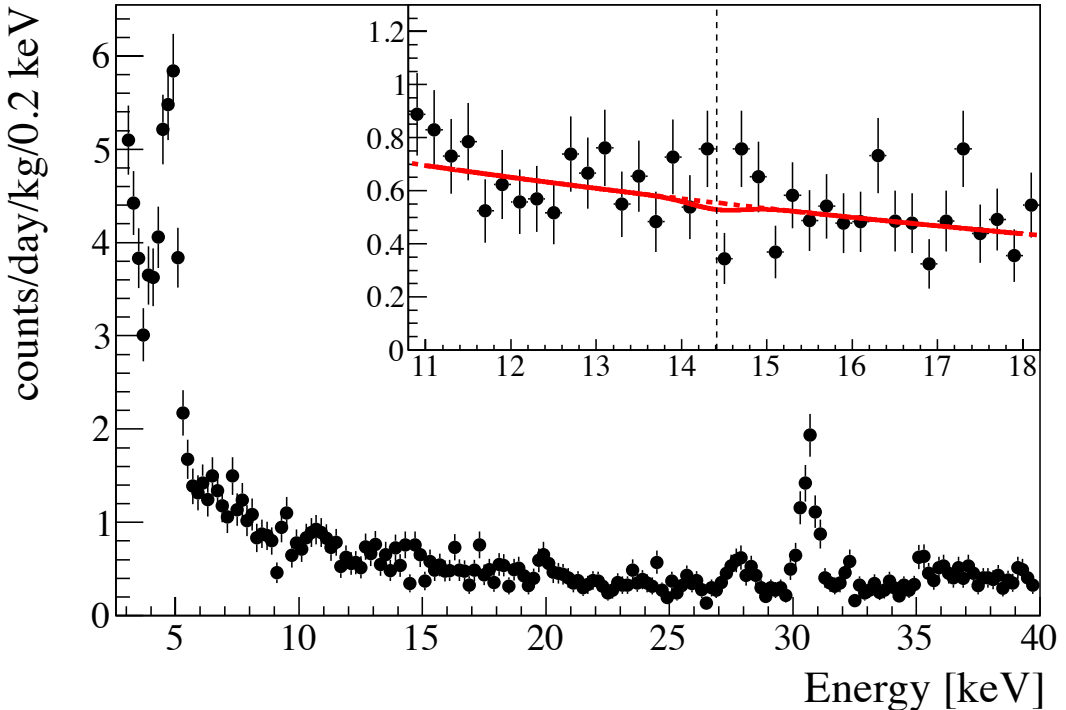


Figure 3. Energy spectrum for the low energy region between threshold and 40 keV. The two peaks at 4.7 keV and 30.49 keV are those used to study the energy resolution at low energy. The axion region around 14.4 keV is magnified in the inset with the fit result shown as red curve. No peak is observed at 14.4 keV, the M1 transition energy of ^{57}Fe for solar axions.

111 As a further check of the calibration, we faced to a bolometer a ^{55}Fe source. The X- rays
 112 produced, with nominal energy between 5.888 and 6.490 keV, were shifted by only 48 ± 16
 113 eV.

114 The energy calibration is obtained from a third degree polynomial fit. The complete low
 115 energy spectrum is modeled with two exponentials, one for the region lower than 5 keV, one
 116 for the background above 7 keV, and also a Gaussian indicative of the peak around 4.7 keV:

$$f_{\text{global}}(E) = \alpha_1 \cdot e^{-\beta_1 \cdot E} + \alpha_2 \cdot e^{-\beta_2 \cdot E} + \frac{\alpha_3}{\sqrt{2\pi}\sigma} e^{\frac{(E-E_{4.7})^2}{2\sigma^2}}. \quad (3.1)$$

117 Extracting the fit parameters obtained using Eq. 3.1 applied to Fig. 3 yields $\sigma_{4.7} = 0.31 \pm 0.04$
 118 keV. This value is then applied to the fit in the axion region from 11 to 18 keV. It is not
 119 as reasonable to extract limits based on the overall global fit since the fluctuation in the
 120 background is more pronounced in the spectrum shown in inset of Fig. 3, the region where
 121 the 14.4 keV axion interaction would be observed.

122 To this spectrum a “modified” fit is applied to extract limits on the axion’s coupling
 123 constant and mass. First, the background needs to be modeled. The background function
 124 appears to be flat, but to ensure validity first, second and third order polynomials are tested
 125 along with an exponential. For each, a Pearson’s- χ^2 test is performed to determine the most

126 accurate background fit. We find that an exponential models the background most accurately,
 127 so this is used with a Gaussian function to represent the 14.4 keV axion peak. The variance for
 128 the Gaussian will be the previously found $\sigma_{4.7}$. The bolometers resolution is not dominated
 129 by signal fluctuations and we know that the energy dependence of the detector resolution is
 130 weak; no significant change is expected from 4.7 keV to 14.4 keV². The signal plus background
 131 model which we have used in the fit is therefore:

$$f_{\text{axion}}(E) = a_1 e^{b \cdot E} + \frac{a_2}{\sqrt{2\pi}\sigma_{4.7}} \text{Exp}\left[\frac{(E - E_{14.4})^2}{2\sigma_{4.7}^2}\right] \quad (3.2)$$

132 No excess in the axion region is observed. We set therefore a lower bound on the axion
 133 decay constant f_a based on the background fluctuations.

134 There are 116 ± 12 counts in the energy interval between $[E_{14.4} - \sqrt{2}\sigma_{4.7}, E_{14.4} + \sqrt{2}\sigma_{4.7}]$,
 135 corresponding to $2.65 \pm 0.27 \text{ c}\cdot\text{kg}^{-1}\cdot\text{d}^{-1}$.

136 Assuming Poisson statistics and including the combined effect of a fluctuation of the
 137 background and of the 15% systematic error induced by cut efficiencies and the uncertainty
 138 in the solar axion rate, we assert that the axion detection rate is $\leq 0.63 \text{ c}\cdot\text{kg}^{-1}\cdot\text{d}^{-1}$ at a 95
 139 % C.L. Using $S=0.55$, this places a bound on the axion coupling constant of $f_a \geq 0.76 \times 10^6$
 140 GeV at 95% C.L.

141 The 95% C.L. and the $1-\sigma$ bounds as a function of the nuclear S parameter are shown
 142 in Fig. 4.

143 4 Summary and Conclusions

144 An experimental search was performed for axions from the solar core from the 14.4 keV
 145 M1 ground-state nuclear transition in ^{57}Fe . The detection technique employed a search for
 146 a peak in the energy spectrum at 14.4-keV when the axion is absorbed by an electron via
 147 the axio-electric effect. The cross section for this process is proportional to the photo-electric
 148 absorption cross section for photons. In this pilot experiment 43.65 kg·d of data were analyzed
 149 resulting in a lower bound on the Peccei-Quinn energy scale of $f_a \geq 0.76 \times 10^6$ GeV for a
 150 value for the flavor-singlet axial vector matrix element of $S=0.55$; bounds are presented in a
 151 graph for values $0.15 \leq S \leq 0.55$.

152 With the numbers quoted in the text, the limit on f_a translates into a mass limit $m_a < 6$
 153 eV, significantly more stringent than in recent results obtained with ^{57}Fe detectors [31] and
 154 by the Borexino experiment [32] [33].

155 The CUORE experiment will have about 740 kg TeO_2 . With live-time of 5 live years
 156 the exposure will be 1.4×10^6 kg·d. With a similar background as the one reported here the
 157 expected sensitivity on f_a will be roughly increased by an order of magnitude.

158 5 Acknowledgments

159 This work was partially supported by NSF Grant 0855-314, DOE Grant W-7405-Eng-48, the
 160 U.S. Department of Energy under Contract No. DE-AC03-76-SF00098, the Istituto Nazionale
 161 di Fisica Nucleare (INFN), and the Commission of the European Community under Contract
 162 No. HPRN-CT-2002-00322. We gratefully acknowledge the kind support of the Laboratori
 163 Nazionali del Gran Sasso. We also warmly thank C. Peña-Garay, A. Serenelli and F. Villante
 164 for useful discussion about solar core ^{57}Fe content.

²We have also checked the resolution at the 30.5 keV X-ray line shown in Table 2, finding a very consistent value.

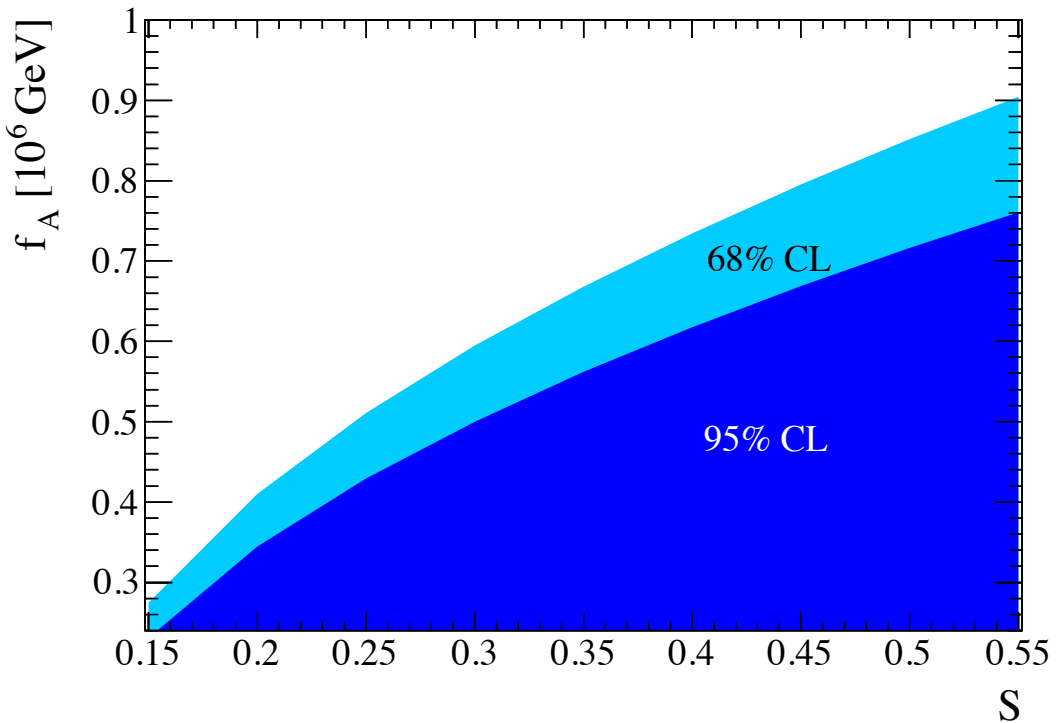


Figure 4. Exclusion plots for one and two sigma confidence levels for f_a as a function of the nuclear S parameter values (see Eq. 1.7 for the meaning of the S parameter).

165 **References**

- 166 [1] C. A. Baker et al., Phys. Rev. Lett. **97** no. 13, 131801 (2006).
- 167 [2] R. D. Peccei and Helen R. Quinn, Phys. Rev. D **16** no. 6, 17911797 (1977).
- 168 [3] S. Weinberg, Phys. Rev. Lett. **40**, 223 (1978); F. Wilczek, Phys. Rev. Lett. **40**, 279 (1978).
- 169 [4] P. Sikivie and Q. Yang, Phys. Rev. Lett. **103**, 111301 (2009).
- 170 [5] J. E. Kim, Phys. Lett. **43**, 103 (1979); M. A. Shifman et al., Nucl. Phys. B **166**, 493 (1980).
- 171 [6] A. R. Zhitnitskiy, Yad. Fiz. **31**, 497 (1980); M. Dine et al., Phys. Lett. B **104**, 199 (1981).
- 172 [7] B. Beltran et al. (CAST Collaboration), PoS **HEP2005** 022 (2006) [arxiv: hep-ex/0507007].
- 173 [8] F. T. Avignone, Phys. Rev. D **79** no. 3, 035015 (2009).
- 174 [9] P. Bandyopadhyay and C.U. Segre www.csrrri.iit.edu/miscal.html.
- 175 [10] A. Serenelli et al., Astrophys. J. **705** L123-L127 (2009).
- 176 [11] S. Moriyama, Phys. Rev. Lett. **75** no. 18, 3222-3225 (1995).
- 177 [12] W. C. Haxton and K. Y. Lee, Phys. Rev. Lett. **66** no. 20, 2557-2560 (1991).
- 178 [13] F. T. Avignone III et al., Phys. Rev. D **37** 618-630 (1988).
- 179 [14] D. Adams et al. (Spin Muon Collaboration), Phys. Rev. D **56** no. 9, 5330-5358 (1997).
- 180 [15] G. Altarelli et al., Nucl. Phys. B **496** no. 1-2, 337-357 (1997).

181 [16] E. Andreotti et al. (Cuoricino Collaboration), Phys. Rev. C **85** 045503 (2012).
182 [17] E Andreotti et al. (Cuoricino Collaboration), Astrop. Phys. **34** 822831 (2011).
183 [18] C. Arnaboldi et al. (Cuoricino Collaboration), Phys. Rev. C **78** 035502 (2008).
184 [19] F. Alessandria et al. (CUORE Collaboration), [arxiv:hep-ex/1109.0494].
185 [20] Arnaboldi et al., Journ. of Crys. Growth, vol. **312**, p. 2999-3008; F. Alessandria et al.
186 [arXiv:nucl-ex/1108.4757]
187 [21] E. Andreotti et al. (CUORICINO Collaboration), Astrop. Phys. **34** 643-648 (2011).
188 [22] M. Redshaw et al., Phys. Rev. Lett. **102** 212-502 (2009).
189 [23] N.D. Scielzo et al., Phys. Rev. **C80** 025501 (2009).
190 [24] S. Di Domizio, PhD Thesis (2009) Dipartimento di Fisica - Università di Genova - Italy
191 [25] S. Di Domizio, F. Orio, and M. Vignati, JINST **6** P02007 (2011).
192 [26] F. Alessandria et al., (CUORE Collaboration) arXiv:1209.2519, submitted to PRD
193 [27] A. Alessandrello et al., Nucl. Instrum. Meth. A **412**, 454 (1998).
194 [28] C. Arnaboldi, G. Pessina, and E. Previtali, IEEE Trans. Nucl. Sci. **50**, 979 (2003).
195 [29] E. Andreotti et al., Nucl. Instr. & Meth. A **664** 161 (2012).
196 [30] M. Carrettoni and M. Vignati, JINST **6**, P08007 (2011).
197 [31] A. V. Derbin et al., Phys. of Atomic Nucl. **74** 596-602 (2011).
198 [32] G. Bellini et al. (Borexino Collaboration) Eur. Phys. J. C **54**, 61-72 (2008).
199 [33] G. Bellini et al. (Borexino Collaboration) Phys. Rev D **85**, 092003 (2012).